J|A|C|S
ARTICLES
Published on Web 07/17/2002

Self-Assembled Nanoparticle Probes for Recognition and Detection of Biomolecules

Dustin J. Maxwell, Jason R. Taylor, and Shuming Nie*,†

Contribution from the Department of Chemistry, Indiana University, Bloomington, Indiana 47405

Received February 5, 2002

Abstract: Colloidal gold nanocrystals have been used to develop a new class of nanobiosensors that is able to recognize and detect specific DNA sequences and single-base mutations in a homogeneous format. At the core of this biosensor is a 2.5-nm gold nanoparticle that functions as both a nano-scaffold and a nano-quencher (efficient energy acceptor). Attached to this core are oligonucleotide molecules labeled with a thiol group at one end and a fluorophore at the other. This hybrid bio/inorganic construct is found to spontaneously assemble into a constrained arch-like conformation on the particle surface. Binding of target molecules results in a conformational change, which restores the fluorescence of the quenched fluorophore. Unlike conventional molecular beacons with a stem-and-loop structure, the nanoparticle probes do not require a stem, and their background fluorescence increases little with temperature. In comparison with the organic quencher Dabcyl (4,4′-dimethylaminophenyl azo benzoic acid), metal nanoparticles have unique structural and optical properties for new applications in biosensing and molecular engineering.

Introduction

The integration of nanotechnology with biology and medicine is expected to produce major advances in molecular diagnostics, therapeutics, molecular biology, and bioengineering.[1−3] Recent advances have led to the development of functional nanoparticles (electronic, optical, magnetic, or structural) that are covalently linked to biological molecules such as peptides, proteins, and nucleic acids.[4−15] Due to their size-dependent properties and dimensional similarities to biomacromolecules,[16−18] these nanobioconjugates are well suited as contrast agents for in vivo magnetic resonance imaging (MRI),[19−21] as long-circulating carriers for drug release/delivery, and as structural scaffolds for tissue engineering.[22,23] In addition, metal and semiconductor colloidal nanoparticles are under intensive study for potential applications in materials synthesis,[12−14,24−26] in multiplexed bioassays,[27,28] and in ultrasensitive optical detection and imaging.[5−7,29−31]

In this report, we show that biomolecules and nanoparticles can be linked to create a novel nanobiotransducer that is able to recognize and detect target biomolecules in a single step (without washing or separation). At the core is a colloidal gold nanocrystal that is both *structurally* and *functionally* integrated

* To whom correspondence should be addressed. E-mail: snie@emory.edu.
† Current address: Departments of Biomedical Engineering, Chemistry, and Oncology, and the Winship Cancer Institute, Georgia Institute of Technology and Emory University School of Medicine, 1639 Pierce Dr., Suite 2001, Atlanta, GA 30322.

(1) LaVan, D. A.; Lynn, D. M.; Langer, R. *Nat. Rev. Drug Discovery* **2002**, *1*, 77−84.
(2) Chan, W. C. W.; Maxwell, D. J.; Gao, X.; Bailey, R. E.; Han, M.-Y.; Nie, S. *Curr. Opin. Biotechnol.* **2002**, *13*, 40−46.
(3) Niemeyer, C. M. *Angew. Chem., Int. Ed.* **2001**, *40*, 4128−4158.
(4) Whaley, S. R.; English, D. S.; Hu, E. L.; Barbara, P. F.; Belcher, A. M. *Nature* **2000**, *405*, 665−668.
(5) Bruchez, M., Jr.; Moronne, M.; Gin, P.; Weiss, S.; Alivisatos, A. P. *Science* **1998**, *281*, 2013−2015.
(6) Chan, W. C. W.; Nie, S. M. *Science* **1998**, *281*, 2016−2018.
(7) Mattoussi, H.; Mauro, J. M.; Goldman, E. R.; Anderson, G. P.; Sundar, V. C.; Mikulec, F. V.; Bawendi, M. G. *J. Am. Chem. Soc.* **2000**, *122*, 12142−12150.
(8) Mitchell, G. P.; Mirkin, C. A.; Letsinger R. L. *J. Am. Chem. Soc.* **1999**, *121*, 8122−8123.
(9) Pathak, S.; Choi, S.-K.; Arnheim, N.; Thompson, M. E. *J. Am. Chem. Soc.* **2001**, *123*, 4103−4104.
(10) Elghanian, R.; Storhoff, J. J.; Mucic, R. C.; Letsinger, R. L.; Mirkin, C. A. *Science* **1997**, *277*, 1078−1081.
(11) Reynolds, R. A., III; Mirkin, C. A.; Letsinger, R. L. *J. Am. Chem. Soc.* **2000**, *122*, 3795−3796.
(12) Mirkin, C. A.; Letsinger, R. L.; Mucic, R. C.; Storhoff, J. J. *Nature* **1996**, *382*, 607−609.
(13) Storhoff, J. J.; Mirkin, C. A. *Chem. Rev.* **1999**, *99*, 1849−1862.
(14) Alivisatos, A. P.; Johnsson, K. P.; Peng, X.; Wilson, T. E.; Loweth, C. J.; Bruchez, M. P., Jr.; Schultz, P. G. *Nature* **1996**, *382*, 609−611.
(15) Dubertret, B.; Calame, M.; Libchaber, A. J. *Nature Biotechnol.* **2001**, *19*, 365−570.
(16) Henglein, A. *Chem. Rev.* **1989**, *89*, 1861−1873.
(17) Schmid, G. *Chem. Rev.* **1992**, *92*, 1709−1727.
(18) Alivisatos, A. P. *Science* **1996**, *271*, 933−937.
(19) Josephson, L.; Tung, C. H.; Moore, A.; Weissleder, R. *Bioconjugate Chem.* **1999**, *10*, 186−191.
(20) Bulte, J. W. M.; Brooks, R. A. Magnetic nanoparticles as contrast agents for MR imaging. In *Scientific and clinical applications of magnetic carriers*; Häfeli, U., Schütt, W., Teller, J., Zborowski, M., Eds.; Plenum Press: New York; 1997; pp 527−543.
(21) Bulte, J. W. M.; Douglas, T.; Witwer, B.; Zhang, S.-C.; Strable, E.; Lewis, B. K.; Zywicke, H.; Miller, B.; van Gelderen, P.; Moskowitz, B. M.; Duncan, I. D.; Frank, J. A. *Nat. Biotechnol.* **2001**, *19*, 1141−1147.
(22) Curtis, A.; Wilkinson, C. *Trends Biotechnol.* **2001**, *19*, 97−101.
(23) Gref, R.; Minamitake, Y.; Peracchia, M. T.; Trubetskoy, V.; Torchilin, V.; Langer, R. *Science* **1994**, *263*, 1600−1603.
(24) Boal, A. K.; Ilhan, F.; Derouchey, J. E.; Thurn-Albrecht, T.; Russell, T. P.; Rotello, V. M. *Nature* **2000**, *404*, 746−748.
(25) Li, M.; Schnablegger, H.; Mann, S. *Nature* **1999**, *402*, 393−395.
(26) Templeton, A. C.; Wuelfing, M. P.; Murray, R. W. *Acc. Chem. Res.* **2000**, *33*, 27−36.
(27) Han, M. Y.; Gao, X.; Su, J. Z.; Nie, S. M. *Nat. Biotechnol.* **2001**, *19*, 631−635.
(28) Nicewarner-Pena, S. R.; Freeman, R. G.; Reiss, B. D.; He, L.; Pena, D. J.; Walton, I. D.; Cromer, R.; Keating, C. D.; Natan, M. J. *Science* **2001**, *294*, 137−141.
(29) Klarreich, E. *Nature* **2001**, *413*, 450−452.
(30) Mitchell, P. *Nat. Biotechnol.* **2001**, *19*, 1013−1017.
(31) El-Sayed, M. A. *Acc. Chem. Res.* **2001**, *34*, 257−264.

10.1021/ja025814p CCC: $22.00

with synthetic oligonucleotides (oligos). In the case of DNA probes labeled with a thiol at one end and a dye at the other, we find that the DNA molecules self-organize into a constrained conformation on the nanoparticle surface, and that the fluorophore is completely quenched by the particle. Upon target binding, the constrained conformation opens and the fluorophore is separated from the particle surface. This structural change generates a fluorescence signal that is highly sensitive and specific to the target DNA.

Previous studied have also used conformational changes and nonradiative energy transfer to develop homogeneous fluorescent biosensors. In particular, Tyagi and Kramer[32,33] developed hairpin-shaped oligonucleotide probes (molecular beacons) for real-time PCR detection and single-nucleotide mutation screening. For small molecules, Hellinga and co-workers[34−37] conjugated allosteric proteins (e.g., maltose binding protein) to fluorescent and electroactive labels. Also being developed are catalytically active DNAs (ribozymes),[38] zinc-finger peptides,[39,40] and signaling aptamers.[41−43] However, these studies are restricted to the optical and electronic properties of traditional organic dyes and lanthanide complexes. Here we demonstrate the use of small metal particles as both a "nano-scaffold" and a "nano-quencher". Such integrated bionanostructures offer important advantages and applications that are not possible with conventional biosensing systems.

Materials and Methods

Synthesis of Gold Colloids. Small gold particles were prepared by chemical reduction of chloroauric acid ($HAuCl_4$). Briefly, about 0.4 mL of a $HAuCl_4$ solution (4% w/w) was added to 100 mL of deionized water containing 0.2 M K_2CO_3. This mixture was cooled to 4 °C in an ice bath, and five aliquots (1 mL each) of a fresh sodium borohydride ($NaBH_4$) solution (10 mM) were sequentially added with rapid stirring. The resulting nanoparticles were characterized by transmission electron microscopy (TEM) and UV−vis absorption. Statistical analysis of the TEM data revealed highly monodispersed particles with an average diameter of 2.5 ± 0.3 nm. The UV−vis spectra showed a well-developed surface plasmon absorption peak at 510 nm, with an extinction coefficient (ϵ) of 6.5×10^5 cm^{-1} M^{-1}.

Preparation of Nanoparticle Probes. Custom oligonucleotides were synthesized with a 3′-thiol (−SH) group and a 5′-fluorophore containing the following sequence: 5′-F-T_6-TAG GAA ACA CCA AAG ATG ATA TTT-T_6-SH-3′, where F is fluorescein or tetramethylrhodamine. The oligos were incubated with gold particles overnight at a ratio of two or three oligos per particle. This ratio was used to ensure that each particle was conjugated to at least one oligo molecule. The oligo−particle conjugates were gradually exposed to 0.1 M NaCl in a PBS buffer over a 16-h period, according to a procedure reported by Mirkin and co-workers.[44] This "aging" step was found to improve the stability and hybridization efficiency of the conjugates. The nanoparticle probes were purified three times by centrifugation at 45 000 rpm for ∼20 min. The final product was a red precipitate, which was resuspended and stored in 10 mM phosphate buffer (pH 7.4).

To determine the number of oligo molecules per particle, mercaptoethanol at 10 mM concentration was used to cleave the sulfur−gold bond and to release all conjugated DNA into solution. The amount of released DNA was measured by fluorescence, and the gold particle concentration was measured by optical absorbance at 510 nm. By dividing the total number of oligo molecules by the total number of nanoparticles, we estimated that there were one or two oligo molecules per particle. Using a similar procedure, we calculated that about 80% of the adsorbed oligos was available for specific hybridization. The remaining 20% of the oligos could be displaced by excess mercaptoethanol but were not available for hybridization. This is most likely caused by a steric hindrance effect which prevents some of the adsorbed oligos from binding to targets.

Hybridization Assays. An aliquot of the nanoparticle probes was diluted to about 10 nM with a hybridization buffer (Sigma, St. Louis, MO). Fluorescence studies showed that the bioconjugated probes were stable under high salt conditions (e.g., 0.5 M NaCl and 2−10 mM $MgCl_2$). A 4-fold molar excess of a complementary target (5′-AAA TAT CAT CTT TGG TGT TTC CTA-3′) was added and was allowed to hybridize for 30−60 min at room temperature. The same protocol and conditions were used for a noncomplementary target (5′-TAC GAG TTG AGA GCA AGC AGA GTT GAG CAT-3′) and a single-base mismatch target (5′-AAA TAT CAT CTT T**T**G TGT TTC CTA-3′). All oligonucleotides (including conventional molecular beacons) were synthesized and purified by Midland Certified Reagent Co. (Midland, TX).

Fluorescence Measurements. Fluorescence spectra were obtained by using a scanning spectrometer (Spex, Edison, NJ) at 490-nm excitation for fluorescein and at 545-nm exictation for tetramethylrhodamine (TMR). For kinetic and time-dependent studies, a series of fluorescence spectra were acquired at 2-min time intervals, and the peak intensity at 565 nm (background subtracted) was plotted as a function of time. For thermodynamic and temperature-dependent studies, the nanoparticle probes were heated, and their fluorescence signals were recorded at 5 °C intervals. At each temperature, the fluorescence intensity was recorded after an equilibration period of 15−20 min.

Results and Discussion

Nanoprobe Design. Nanoparticle DNA probes were designed by using small gold nanocrystals and fluorescently labeled oligonucleotides. An important insight came from previous surface-enhanced Raman scattering (SERS) studies, which showed that fluorescent dyes could reversibly adsorb on the surface of colloidal silver and gold nanoparticles.[45,46] Thus, when an oligonucleotide molecule is firmly tethered to a particle (via a sulfur−metal bond), the fluorophore at the distal end can loop back and adsorb on the same particle. Because the backbone of single-stranded DNA is conformationally flexible, a favorable conformation for the adsorbed oligos is an arch-like structure, in which both the 3′- and 5′-ends are attached to the particle but the DNA chain does not contact the surface. Figure 1 shows a schematic diagram of the nanoparticle probes and their operating principles for DNA recognition and detection. In addition to this "arch" structure, there are other surface configurations for the absorbed oligo molecules, but these

(32) Tyagi, S.; Kramer, F. R. *Nat. Biotechnol.* **1996**, *14*, 303−308.
(33) Tyagi, S.; Bratu D. P.; Kramer, F. R. *Nat. Biotechnol.* **1998**, *16*, 49−53.
(34) Marvin, J. S.; Corcoran, E. E.; Hattangadi, N. A.; Zhang, J. V.; Gere, S. A.; Hellinga, H. W. *Proc. Natl. Acad. Sci. U.S.A.* **1997**, *94*, 4366−4371.
(35) Marvin, J. S.; Hellinga, H. W. *J. Am. Chem. Soc.* **1998**, *120*, 7−11.
(36) Benson, D. E.; Conrad, D. W.; de Lorimer, R. M.; Trammell, S. A.; Hellinga, H. W. *Science* **2001**, *293*, 1641−1644.
(37) Marvin, J. S.; Hellinga, H. W. *Proc. Natl. Acad. Sci. U.S.A.* **2001**, *98*, 4955−4960.
(38) Lu, Y.; Li, J. *J. Am. Chem. Soc.* **2000**, *122*, 10466−10467.
(39) Walkup, G. K.; Imperiali, B. *J. Am. Chem. Soc.* **1996**, *118*, 3053−3054.
(40) Godwin, H. A.; Berg, J. M. *J. Am. Chem. Soc.* **1996**, *118*, 6514−6515.
(41) Jhaveri, S. D.; Kirby, R.; Conrad, R.; Maglott, E. J.; Bowser, M.; Kennedy, R. T.; Glick, G.; Ellington, A. D. *J. Am. Chem. Soc.* **2000**, *112*, 2469−2473.
(42) Stojanovic, M. N.; de Prada, P.; Landry, D. W. *J. Am. Chem. Soc.* **2000**, *122*, 11547−11548.
(43) Stojanovic, M. N.; de Prada, P.; Landry, D. W. *J. Am. Chem. Soc.* **2001**, *123*, 4928−4931.
(44) Demers, L. M.; Mirkin, C. A.; Mucic, R. C.; Reynolds, R. A., III; Letsinger, R. L.; Elghanian, R.; Viswanadham, G. *Anal. Chem.* **2000**, *72*, 5535−5541.
(45) Nie, S. M.; Emory, S. R. *Science* **1997**, *275*, 1102−1106.
(46) Krug, J. T.; Wang, J. D.; Emory, S. R.; Nie, S. M. *J. Am. Chem. Soc.* **1999**, *121*, 9208−9214.

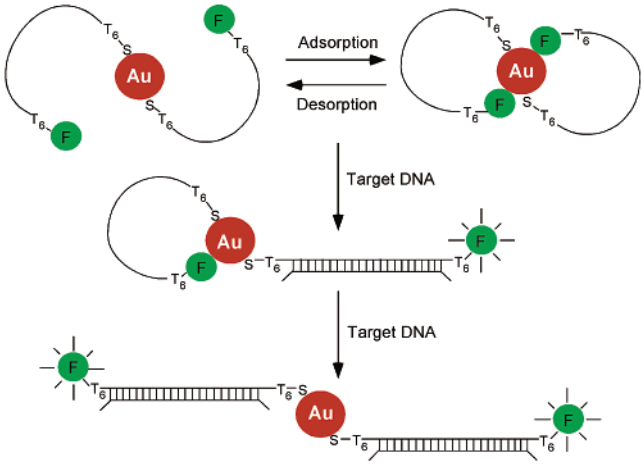

Figure 1. Nanoparticle-based probes and their operating principles. Two oligonucleotide molecules (oligos) are shown to self-assemble into a constrained conformation on each gold particle (2.5 nm diameter). A T_6 spacer (six thymines) is inserted at both the 3′- and 5′-ends to reduce steric hindrance. Single-stranded DNA is represented by a single line and double-stranded DNA by a cross-linked double line. In the assembled (closed) state, the fluorophore is quenched by the nanoparticle. Upon target binding, the constrained conformation opens, the fluorophore leaves the surface because of the structural rigidity of the hybridized DNA (double-stranded), and fluorescence is restored. In the open state, the fluorophore is separated from the particle surface by about 10 nm. See text for detailed explanation. Au, gold particle; F, fluorophore; S, sulfur atom.

configurations would not be able to recognize specific DNA sequences (the oligo structures and quenching mechanisms are discussed in detail in a later section).

This constrained conformation leads to three important results: (i) the fluorophore is completely quenched by efficient nonradiative energy transfer to the gold particle;[47,48] (ii) the exposed oligo sequence is available for specific hybridization; and (iii) the hybridization specificity is expected to be higher than that of linear probes. The latter point comes from previous studies by Libchaber, Kramer, and co-workers,[49] which reveal that conformationally constrained probes offer higher hybridization specificities than linear probes. This improvement is due to an intermediate state that is able to compete with the fully hybridized state as well as with the denatured, random-coil state. In the case of gold colloids, molecular "looping" on the particle surface leads to a bent DNA conformation that acts as an intermediate state to increase the hybridization specificity.

Upon target binding, the constrained conformation is opened and the fluorophore is separated from the particle surface. Similar to the case with molecular beacons,[32,33] this structural change arises from a dramatic increase in the DNA rigidity after hybridization (becoming double-stranded). For signal generation in the nanoparticle probes, two factors must be considered. First, the surface adsorption energies of organic dyes on silver and gold are usually in the range of 8−16 kcal/mol,[50] which are considerably smaller than the energies (ΔH = 80−100 kcal/mol) involved in DNA hybridization. Target binding to self-assembled oligo probes (20−24 bases) should thus result in a separation (desorption) of the fluorophore from the surface. Second, nonradiative energy transfer from an excited molecule to a gold particle is a relatively short-range (1−2 nm) effect when the particles are small (2−3 nm).[47,48]

We also note that molecular recognition comes only from the attached ligands, but the gold nanocrystals serve an important structural role in interacting with both the thiol group and the fluorophore that are attached to the two ends of an oligonucleotide molecule. This interaction occurs on the nanometer scale and is essential for organizing the oligos into an arch-like conformation on the particle surface.

Quenching Mechanisms. To understand the mechanisms of fluorescence quenching, it is important to first consider whether Ag or Au nanoparticles should be treated as a conventional quencher and whether the standard Förster formula could be used to calculate the energy-transfer efficiencies. In the case of resonant surface-plasmon excitation, a small dipole in the excited fluorophore induces a large dipole in the particle, leading to an enhancement in the energy-transfer efficiencies. Electromagnetic field calculations suggest that surface plasmon resonances can enhance the energy-transfer rates by as much as 10^4−10^5 if a metal particle is placed between a donor and an acceptor.[51] The calculated energy-transfer distances are as large as 70−100 nm, about 10 times longer than the typical Förster distances (R_o).[52] On the other hand, it is well known that surface plasmon excitation can dramatically increase the electromagnetic field near the particle surface, leading to surface-enhanced Raman scattering and surface-enhanced fluorescence emission.[53,54]

Because of these complicating factors, we decided to investigate experimentally how fluorophores would interact with gold nanoparticles. When not conjugated to oligo DNA, many organic fluorophores such as rhodamine 6G and tetramethylrhodamine are completely quenched by gold nanoparticles (Figure 2A, black curve). This is not surprising because previous studies have shown that most fluorescent dyes spontaneously adsorb on gold and silver surfaces.[45,46,50] In fact, Hildebrandt and Stockburger[50] have estimated that the binding equilibrium constant between R6G and silver is about 10^9. A different behavior was observed when the fluorophore was linked to an oligonucleotide, because the negative charges on the oligonucleotide appeared to interfere with fluorophore adsorption on the particle surface (also negatively charged). Our experimental data showed a quenching efficiency of 55% when the fluorophore was not adsorbed on the particle (dynamic quenching) and a quenching efficiency of nearly 100% when the fluorophore was statically adsorbed on the particle (static quenching) (Figure 2B). For efficient surface adsorption, it was necessary to use Mg^{2+} ions to neutralize the negative charges on the DNA chain. In comparison with colloidal gold, the organic quencher Dabcyl[31,32] caused less than 5% quenching under identical conditions (that is, same fluorophore, quencher, and salt concentrations). Clearly, the stronger quenching abilities of colloidal gold are related to its large molar extinction coefficients (6.5×10^5 cm^{-1} M^{-1} for 2.5-nm particles) and its nanomolar binding affinities for organic dyes.

Complete fluorescence quenching was also observed for rhodamine 6G and fluorescein in the presence of 1−2 mM divalent cations. This result suggests that a positive charge on

(47) Pineda, A. C.; Ronis, D. *J. Chem. Phys.* **1985**, *83*, 5330−5337.
(48) Pockrand, I.; Brillante, A.; Mobius, D. *Chem. Phys. Lett.* **1980**, *69*, 499−504.
(49) Bonnet, G.; Tyagi, S.; Libchaber, A.; Kramer, F. R. *Proc. Natl. Acad. Sci. U.S.A.* **1999**, *96*, 6171−6176.
(50) Hildebrandt, P.; Stockburger, M. *J. Phys. Chem.* **1984**, *88*, 5935−5844.
(51) Gersten, J. I.; Nitzan, A. *Surf. Sci.* **1985**, *158*, 165−189.
(52) Stryer, L. *Annu. Rev. Biochem.* **1978**, *47*, 819−846.
(53) Moskovits, M. *Rev. Mod. Phys.* **1985**, *57*, 783−826.
(54) Sokolov, K.; Chumanov, G.; Cotton, T. M. *Anal. Chem.* **1998**, *70*, 3898−3905.

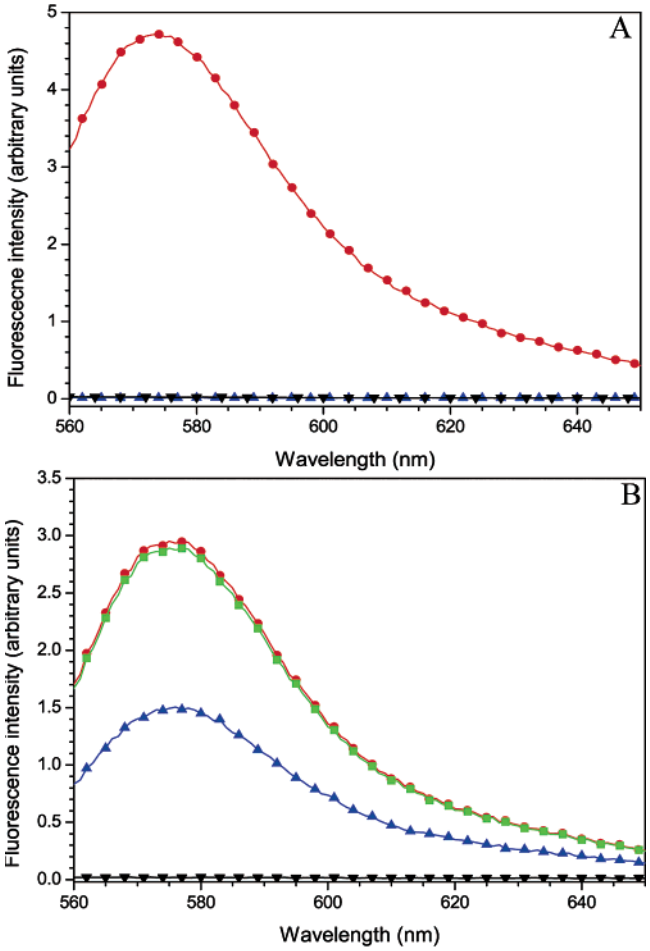

Figure 2. Spontaneous adsorption of fluorophores on gold particles and complete fluorescence quenching. (A) Fluorescence spectra obtained from 0.1 μM TMR (free dye) under the following conditions: without a quencher (red curve), with 2 μM gold nanoparticles (black curve), and after the gold particles were removed by centrifugation (complete adsorption, no dye left in solution) (blue curve). (B) Fluorescence spectra obtained from 0.1 μM TMR-labeled DNA (5′-TMR-T_6-TAG GAA ACA CCA AAG ATG ATA TTT-3′, not thiolated) under the following conditions: without a quencher (red curve), with 2 μM Dabcyl (5% quenching, green curve), with 2 μM gold particles (55% dynamic quenching, blue curve), and with 2 μM gold nanoparticles plus 2.0 mM $MgCl_2$ (100% static quenching, black curve). Note that the oligos do not have an anchoring thiol group and are different from the thiolated probes shown in Figure 3.

the fluorophore is not required for adsorption on gold particles. In fact, both fluorecein and colloidal gold are expected to be negatively charged at neutral pH and should thus repel each other by electrostatic forces. The quenching results show that the use of a small amount of divalent cations such as Mg^{2+} allows the adsorption of charged fluorophores and oligonucleotides on gold nanoparticles.

Single-Base Mismatch Detection. The nanoparticle probes are highly specific in discriminating against noncomplementary DNA sequences and single-base mismatches. The addition of noncomplementary nucleic acids had no effect on the fluorescence, and a single-base mismatch reduced the fluorescence intensity by 55% (in comparison with the fluorescence intensity of perfectly matched targets) (Figure 3). However, a weak and broad background was observed mainly because our current purification protocols did not completely remove the aggregated particles (light scattering) and the free/unquenched oligos (residual fluorescence). Slow mercapto desorption could also

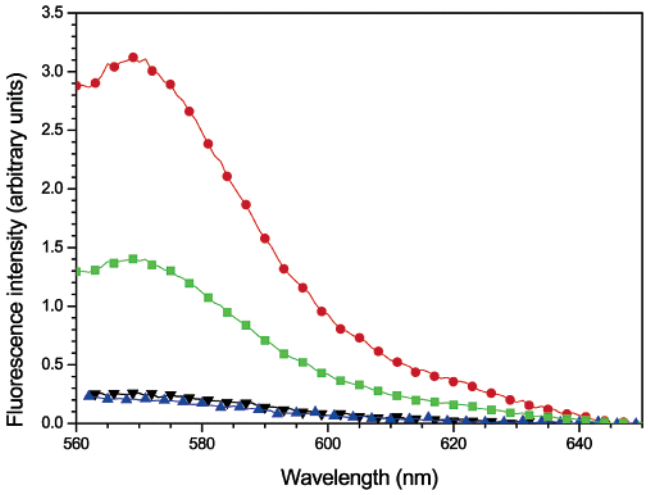

Figure 3. Fluorescence spectra demonstrating detection of specific DNA sequences and single-base mismatches using nanoparticle probes. Red curve, perfectly complementary target (5′-AAA TAT CAT CTT TGG TGT TTC CTA-3′); green curve, single-base mismatch (5′-AAA TAT CAT CTT T**T**G TGT TTC CTA-3′); blue curve, noncomplementary target; and black curve, control probes (no added target). Similar results are observed by using either TMR or fluorescein as the fluorophore. Detailed conditions are described in the Experimental Section.

contribute to the background, but this problem was minimized by using fresh nanoparticle probes (used within 24 h of preparation).

The sequence specificities achieved with nanoparticle probes are similar to or slightly lower than those of molecular beacons, for which single-base mismatches result in a 50−90% signal decrease.[31,32,55] Recently, Dubertret et al.[15] also achieved single-base mismatch detection and efficient quenching (up to 99.96% under favorable conditions) by replacing Dabcyl with 1.4-nm gold clusters (nanogold). However, they followed the traditional molecular beacon design and used hairpin-shaped oligonucleotides for hybridization.[31,32] Their nanogold clusters are too small to develop surface plasmon resonances, and the gold−DNA linkage is unstable under the temperature cycling conditions of PCR.

Kinetics and Thermodynamics. In comparison with previous work,[15] our nanoparticle probes are based on a different design, and their kinetic and thermodynamic properties are fundamentally different from those of molecular beacons. As shown in Figure 4A, the probe-opening rate cannot be fit by a single exponential, and the curve exhibits a rapid jump in the first 5 min and a slow increase over a 45−50-min period. As measured by the fluorescence intensity, the fast jump component corresponds to ~40% of the adsorbed oligos. The remaining component (~60%) shows a slower response than molecular beacons.

There are several possible reasons for the slow hybridization kinetics. One possibility is that the strong affinities of fluorophore binding to the particle surface would reduce the rates of hybridization and loop opening, similar to the slow binding kinetics observed for molecular beacons with long stems.[56] Here, the reduced binding kinetics would be accompanied by an increase in the target binding specificity. However, the binding specificities of our nanoparticle probes are not significantly

(55) Liu, X.; Tan, W. *Anal. Chem.* **1999**, *71*, 5054−5059.
(56) Bao, G.; Tsourkas, A., presented at the SPIE−Photonics West Meeting, San Jose, CA, January 21−24, 2002.

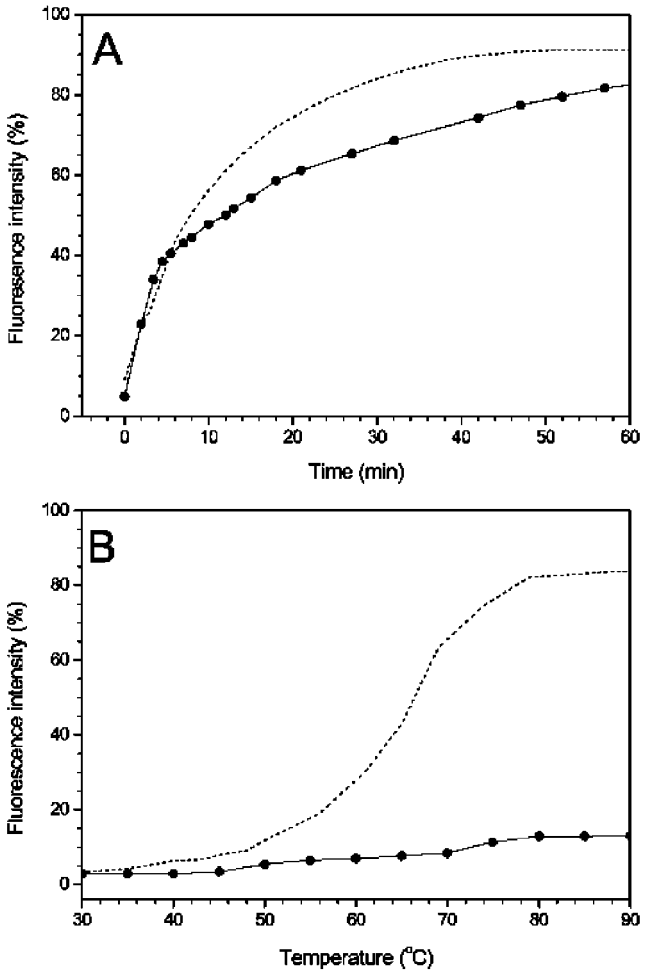

Figure 4. Kinetic and thermodynamic properties of the nanoparticle probes. (A) Plots of fluorescence signal as a function of time for nanoparticle probes (solid line) and molecualr beacons (dotted line). (B) Effects of temperature on fluorescence for nanoparticle probes (solid line) and molecular beacons (dotted line). Kinetic data were obtained by using a complementary target, and temperature data were obtained from the nanoprobes themselves (no added target). The beacon sequence was the same as that of the nanoprobes, except that the T_6 spacer was replaced by a self-complementary stem.

higher than those of molecular beacons. On the basis of this argument, one can conclude that fluorophore adsorption is not responsible for the slow hybridization kinetics. A less obvious but more plausible explanation is that the surface-bound oligos are less accessible for hybridization, due to less favorable steric and electrostatic factors. For example, a portion of the adsorbed oligos may not be immediately available for hybridization, and the slow kinetics could be the result of a slow configuration change for these oligos. In this case, surface modifications using alkane thiols or thiolated poly(ethylene glycol)s (forcing the oligos to adopt a single conformation) should improve the binding kinetics.

A novel feature is that the nanoparticle probes and molecular beacons respond to temperature in different fashions. Molecular beacons open around their melting temperatures ($T_m = 65-70$ °C), but the nanoparticle probes undergo little or no conformational changes as a function of temperature (Figure 4B). This unusual behavior suggests that surface adsorption is much less dependent on temperature than DNA melting. Consistent with this view, recent SERS studies indicate that rhodamine 6G molecules are stably adsorbed on silver surfaces at temperatures as high as 80−100 °C (W. Doering and S. Nie, unpublished data). This temperature stability allows the use of these probes in real-time PCR studies under normal temperature-cycling conditions (detailed results to be published elsewhere). This lack of temperature dependence, however, does not mean that the signal-to-noise ratios would be better at higher temperatures. In fact, the signal-to-noise ratios will deteriorate above the DNA melting temperature because efficient hybridization between the target and the probe cannot occur under such conditions.

Surface Configurations of Adsorbed Oligos. A key remaining question is the role of the terminal thiol group and the surface structures of the adsorbed oligo molecules. In Figure 2, we have shown that a thiol group is not essential for surface adsorption, because efficient fluorescence quenching is observed as long as there is a certain amount of divalent cations (e.g., 2−5 mM Mg^{2+}) in the hybridization buffer. However, without a tethering thiol, the adsorbed oligos do not assemble into the appropriate conformation and cannot recognize specific DNA sequences. As shown in Figure 5A, the nonthiolated probes exhibit no sequence discrimination, and both complementary and noncomplementary targets produce similar fluorescence signals. In fact, we found that any oligo molecules could displace the adsorbed oligos and release them into solution simply by mass action (Figure 5B). In contrast, the thiol-labeled oligos remain on the particle surface after hybridization, and the supernatant solution shows little or no fluorescence (black curve in Figure 5B). One explanation for this dramatic difference is that oligo molecules lacking an anchoring thiol group adopt a nonspecific, flat configuration on the particle surface, with divalent cations acting as a bridge between the oligo and the particle. For oligonucleotides with a terminal thiol group, this flat geometry becomes less stable than a standing or bent configuration.

In Figure 6 are shown two possible configurations for a nonthiolated oligo (A) and four possible configurations for a thiolated oligo (B). For the nonthiolated probes, the standing configuration would not work because it does not generate a fluorescence signal after hybridization (the fluorophore remains quenched); the flat configuration would not work either, because it is not sequence specific (both complementary and noncomplementary DNA can replace the adsorbed oligos and can generate a fluorescence signal). For the thiolated probes, the flat configuration is not available for target binding because of a steric blocking effect (the oligo is wrapped around the particle). In fact, this geometry is likely to represent the population (∼20%) of adsorbed oligos that cannot hybridize with target DNA but can be displaced by another thiol such as mercaptoethanol. The "arch" configuration is expected to rapidly respond to specific sequences and to generate a fluorescence signal, perhaps corresponding to the initial signal jump (∼40% of the total fluorescence). The "stretched arch" configuration should also be available for specific hybridization, but it exhibits more tension and steric hindrance that should reduce the hybridization kinetics. It is thus likely that this stretched structure corresponds to the slow kinetic component (∼60% of the total fluorescence), as observed in Figure 4A. The last configuration will not produce a fluorescence change but will contribute to the fluorescence background. To optimize the detection sensitivity of the gold nanoparticle probes, it is important that this standing configuration be minimized in the future.

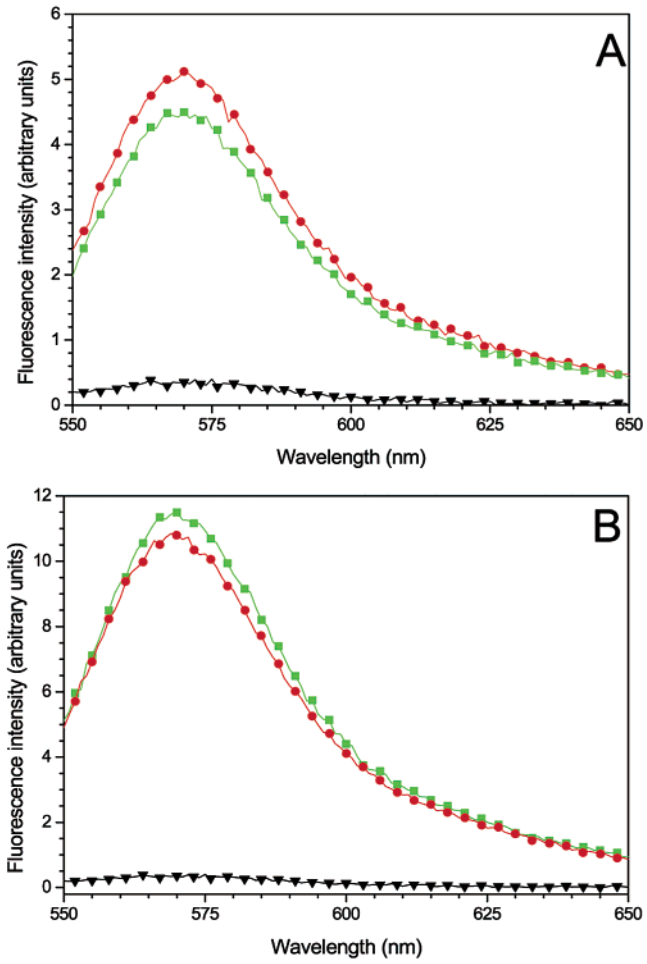

Figure 5. Fluorescence responses and the lack of sequence recognition abilities observed for nonthiolated nanoparticle probes. (A) Fluorescence spectra of nonthiolated probes generated by a complementary target (red curve), a noncomplementary target (green curve), and no target (black curve). These probes are considered nonfunctional because they do not recognize specific DNA sequences. (B) Fluorescence signals obtained from the supernatant solution when the probes were treated with a complementary target (red curve) or a noncomplementary target (green curve). The result revealed that the oligos were released into solution by nonspecific adsorption of the target on the particle surface. With a thiol group, this release was not observed (little or no signal in solution, black curve in B). The nonfunctional probes were prepared in the same way as the functional probes, except that the 3′-end thiol group was deleted. The intensity differences for the red and green curves were within experimental errors and had no particular significance.

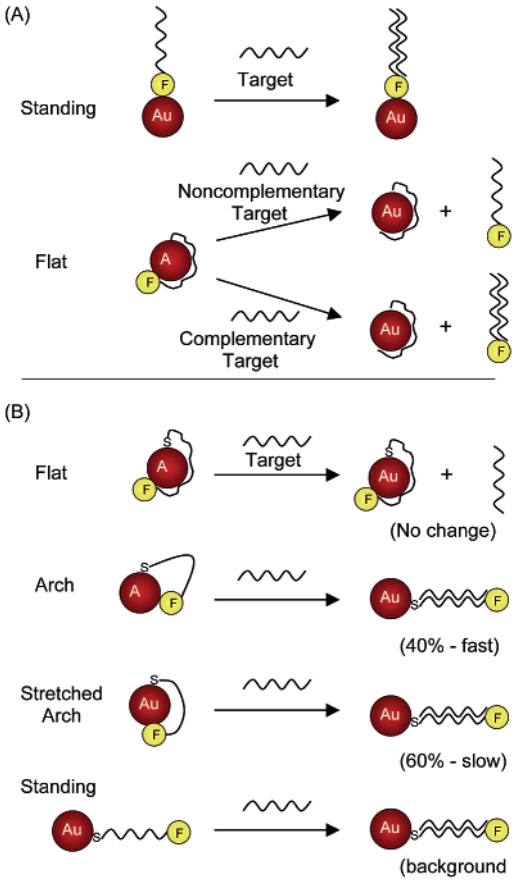

Figure 6. Schematic illustration of possible configurations for (a) nonthiolated and (b) thiolated oligonucleotides adsorbed on colloidal gold nanocrystals. Detailed discussion in text.

Previous studies have reported a number of configurations for adsorbed oligos under certain conditions. For example, Mirkin and co-workers[44] reported a low "aging" procedure in which mercaptoalkyl oligo molecules are believed to change from a flat to a standing configuration on the surface of gold particles. Only the standing configuration is available for specific DNA hybridization. Murphy, Herne, and their co-workers have shown that single-stranded DNA molecules can nonspecifically adsorb on gold thin films and semiconductor nanoparticles in a flat configuration.[57,58] These oligo molecules are not available for hybridization. Furthermore, Emory has used single-molecule and single-particle SERS to study the adsorption geometry of fluorophore-labeled oligos; the results show preferential enhancement of the fluorophore and carbon−sulfur modes, with little or no enhancement of the nucleotide signals.[59] Considering the strong distance-dependence effect of surface-enhanced Raman scattering, this work suggests that the sulfur and the fluorophore groups are in direct contact with the surface, while the DNA bases are separated from the particle surface, as would be expected from an arch-like DNA conformation.

Conclusions

We have demonstrated the design and feasibility of bioconjugated gold nanoparticles for recognizing and detecting specific DNA sequences in a single step. At the present level of development, the hybridization kinetics of the nanoparticle probes is slower than that of conventional molecular beacons, and their sequence specificity and fluorescence enhancement are comparable or slightly lower. However, gold nanocrystals represent a new class of universal fluorescence quenchers that are substantially different from Dabcyl and should find applications in molecular engineering and biosensor development. For small gold nanoparticles, we have shown that an arch-like structure can be assembled on the particle surface and that this structure is not sensitive to temperature, in contrast to the behavior of stem-loop molecular beacons. For relatively large gold particles (10−50 nm diameter), preliminary results demonstrate an efficient long-range energy-transfer effect that is able

(57) Mahtab, R.; Hydrick-Harden, H.; Murphy, C. J. *J. Am. Chem. Soc.* **2000**, *122*, 14−17.
(58) Herne, T. M.; Tarlov, M. J. *J. Am. Chem. Soc.* **1997**, *119*, 8916−8920.
(59) Emory, S. R. Probing single molecules and single nanoparticles with surface-enhanced Raman scattering. Ph.D. Dissertation, Indiana University, Bloomington, IN, 1999, Chapter 3, pp 39−54.

to quench fluorophores over spatial distances as large as 10−20 nm (data not shown). This long-range feature could allow the development of biosensors and homogeneous bioassays that are not possible by using Dabcyl. For example, gold particles could be conjugated to peptide and small-molecule substrates for real-time measurement of the catalytic (e.g., bond cleavage) activities of many enzymes such as HIV proteases[60] and matrix metalloproteiases (MMP)[61,62] as well as the proteins involved in cellular apoptosis.[63]

The methods and principles presented here can be applied to in-vitro-selected aptamers[39−43] for recognizing and detecting a wide range of analytes such as small organic molecules and divalent cations (e.g., zinc and cadmium ions).[34−37] In addition to using metal nanoparticles as quenchers, multicolor semiconductor nanocrystals could be used as "nano-emitters" for multiplexed and real-time PCR. These nanoparticle-based probes offer unique advantages and capabilities that are not available from traditional molecular systems. We envision that multifunctional or smart nanostructures could be developed by conjugating both DNA and proteins to nanoparticles (enough surface area for multiple biomolecules). The attached proteins or peptides should guide nanostructures to specific cells (e.g., cancer cells) or to specific locations inside a cell (where the oligos will detect messenger RNA and the attached signaling peptides will deliver the particles into the nucleus or other locations). Moreover, self-assembled biomolecular sensors could be integrated with microfabricated devices for on-chip detection and monitoring.

Acknowledgment. This work was supported by grants from the National Institutes of Health (R01 GM58173) and the Department of Energy (DOE FG02-98ER14873). S.N. acknowledges the Whitaker Foundation for a Biomedical Engineering Award and the Beckman Foundation for a Beckman Young Investigator Award.

JA025814P

(60) Matayoshi, E. D.; Wang, G. T.; Krafft, G. A.; Erickson. J. *Science* **1990**, *247*, 954−958.
(61) Massova, I.; Kotra, L. P.; Fridman, R.; Mobashery, S. *FASEB* **1998**, *12*, 1075−1095.
(62) Bremer, C.; Tung, C. H.; Weissleder, R. *Nat. Med.* **2001**, *7*, 743−748.
(63) Reed, J. C. *Nat. Rev. Drug Discovery* **2002**, *1*, 111−121.